Sensor and Simulation Notes

Note 580

25 October 2018

HPEM Environment Capabilities at armasuisse in Switzerland

Dr. D. V. Giri, Pro-Tech, Wellesley, MA
Dept. of ECE, University of New Mexico, Albuquerque, NM, USA

Dr. F. M. Tesche, EM Consultant (Retired), USA

Dr. Armin Kälin, formerly with armasuisse, now with EMProtec, Switzerland

and

Mr. Markus Nyffeler, Mr. Pierre Bertholet (Retired)
Dr. Peter Merki and Dr. Carlos Romero
armasuisse, Thun, Switzerland

Abstract

*This note provides a compilation of the available High-Power Electromagnetic (HPEM) environment simulation capabilities at the **armasuisse** HPE Laboratory, Spiez. We have briefly described the source and antenna systems and have plotted the spectral magnitude of the electric field at representative observation points.*

The HPEM systems at the HPE Laboratory consist of: a) nuclear electromagnetic pulse simulators (ex: VEPES and VERIFY), b) moderate-band systems (ex: switched oscillators at 200 MHz and 500 MHz working into helical antennas), c) hyperband systems (ex: HYPS and FID pulsers, which provide transient energy to full and half impulse radiating antennas, and d) a narrowband system (ex: a magnetron source at 2.4 GHz working into a pyramidal horn and a paraboloidal reflector antenna). These Swiss HPEM environment simulation capabilities are also compared with a few standardized spectral magnitudes of electromagnetic field environments.

1. Introduction

In 2004, a paper in the IEEE EMC Transactions [1] described several ways of characterizing high power electromagnetic (HPEM) environments. A qualitative classification approach was to list potential HPEM threat environments based on the *level of sophistication* of the underlying technologies involved in producing the EM environment, such as low, medium and high-tech systems. An alternate classification method was to describe the effects that the HPEM environment can have on a targeted system.

A more quantitative characterization approach that was described in [1] was to describe the environment by its frequency domain (spectral) bandwidth. In this method, four different categories of the environment were defined: narrow band, moderate band, ultra-moderate band and hyperband. An examination of the *percent bandwidth (pbw)* or the *band ratio (br)* of the spectrum of a signal would determine in which category the signal should fall. Table 1, taken from [1], defines the *pbw* and *br* quantities, as well as the four bands.

Table 1. Bandwidth designations for various types of HPEM waveforms, as developed by Giri [1].

	IEME CLASSIFICATION BASED ON BANDWIDTH	
Band type	**Percent bandwidth** $pbw = 200\left(\dfrac{br-1}{br+1}\right)$ (%)	**Bandratio** *br*
Narrow or hypoband	$< 1\%$	< 1.01
Moderate or mesoband	$1\% < pbw \leq 100\%$	$1.01 < br \leq 3$
Ultra-moderate or sub-hyperband	$100\% < pbw < 163.4\%$	$3 < br \leq 10$
Hyperband	$163.4\% < pbw < 200\%$	$br \geq 10$

To better visualize the spectral contents of HPEM environments, ref. [1] suggested the use of a plot the various HPEM spectra as a function of frequency, as originally done by Giri and Kälin [2]. This spectral plot is shown below in Figure 1, and it provided only estimates for the frequency ranges of the environments with no spectral magnitude levels provided. It was designed only to be a rough comparison of the various spectra.
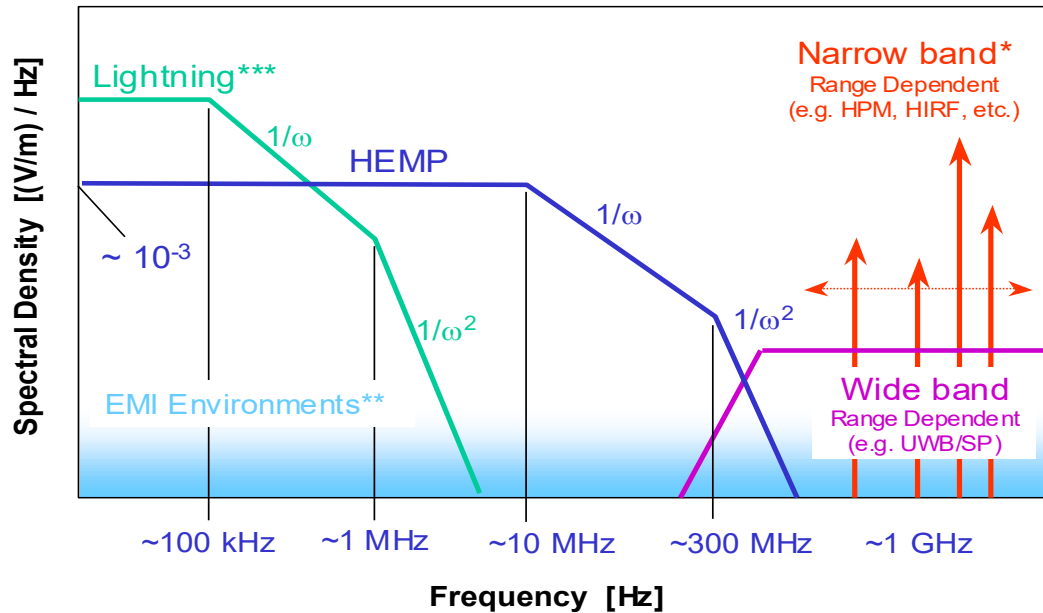
Figure 1.   Early comparison of the spectra of several types of HPEM environments. (From ref. [2].)

The spectral plot of Figure 1 was updated in 2007 by carefully computing the spectral amplitudes and the frequencies of the various HPEM environments and by including several other current-day HPEM sources [3]. The revision of this spectral plot is shown later in Section 3 of this report.

Notably lacking in the revised HPEM environment chart was the fact that the HPEM environments produced by the electromagnetic pulse (EMP) simulators and other HPEM sources available at the **armasuisse** HPE Laboratory were not included. Thus, the authors of this report have been tasked to update this environments chart to include these HPE Laboratory sources, and to compare their environments to those produced by other HPEM sources and facilities.

In Section 2, we have reviewed the various HPEM systems that exist at the HPE Laboratory in Spiez. The spectral magnitudes of the electric fields produced by these systems at selected points of observations are included individually. In Section 3, these Swiss HPEM environments are compiled into a single chart, and presented together with the earlier 2007 chart of worldwide sources.

2. Review of HPEM Sources at the HPE Laboratory

2.1 Guided Wave EMP Simulators

2.2 VEPES

      VEPES is an acronym for *vertically polarized EMP simulator*. This simulator is a guided-wave structure that produces a transient EM field with a waveform similar to that arising from a high-altitude EMP. We refer to this class of simulators as "guided wave" as opposed to "bounded wave", since there is a leakage of electromagnetic fields from the simulator in all directions. For example, high frequencies in the pulse get radiated axially out, very low frequencies go behind the pulser and some of the intermediate frequencies leak out to the sides of the simulator.

      The working volume of this particular simulator, along with a typical test object, is shown in Figure 2.

Figure 2. View of the wave-guiding structure and working volume of the Swiss VEPES simulator.

      Ref. [4] describes the physical and electrical characteristics of this facility as of 2002, which can be summarized as follows

Table 2. Properties of the VEPES Simulator.

Design and construction:	1991
Upgraded (Antenna):	2005 to 2007
Pulser Output Voltage:	250 – 850 kV
Rise Time:	~2.5 ns
Original Pulse Width (FWHM):	~ 23 ns
Polarity:	positive
Electric Field max.:	150 kV/m
Magnetic Field max.:	400 A/m
Test Volume:	8 x 8 x 4 m
Pulse Repetition Rate:	1/min
Termination Resistance:	90 Ω
Dimensions L x B x H:	45 x 18 x 9m
Standard:	MIL-STD-461G RS 105
Insulation / Gas:	Oil / Air, SF_6

In the 2005 to 2007 time period, the structure of the VEPES simulator was upgraded to provide enhanced mechanical stability. Figure 3, taken from ref. [5], presents a typical VEPES waveform in time and frequency domains. There is no significant change in the environment before and after the upgrade, since the upgrade addressed exclusively mechanical issues and preserved the electromagnetic performance of the NEMP simulator.
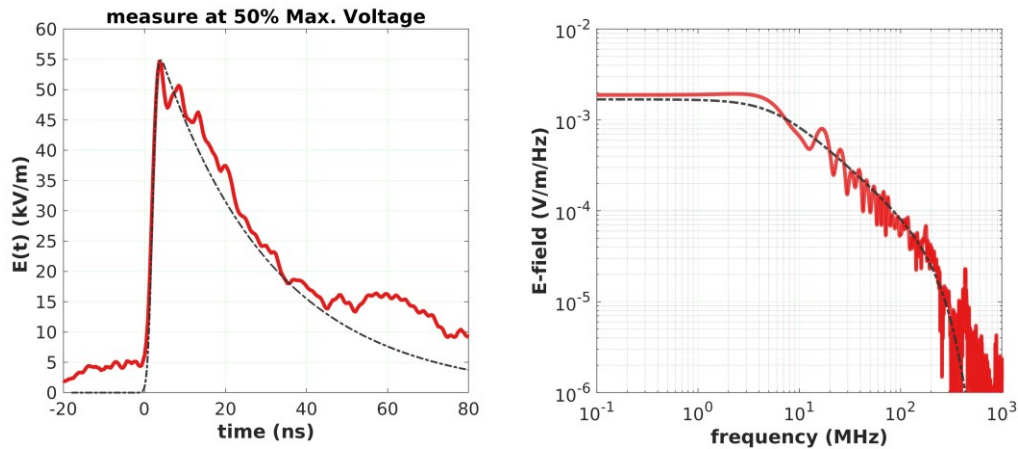
Figure 3.   Illustration of a typical VEPES transient waveform after the upgrade (red) compared with RS 105 waveform (black)

2.3 VERIFY

The vertical indoor facility (VERIFY) is a bounded-wave simulator that produces a transient EM field that is similar to that arising from a HEMP, but with a very fast rise time. Its characteristics are also described in the IEC simulator compendium document [4].

As the name suggests, this simulator is located inside a wooden building in Spiez, and testing is unaffected by the weather outside. Figure 4 provides a view of the working volume of the simulator, which is smaller than in the VEPES facility.

Figure 4.   View of the pulser and working volume of the VERIFY simulator.

Table 3.   Properties of the VEPES Simulator (From ref. [4]).

Design and build:	1999
Pulse Generator Output Voltage:	150 – 500 kV
Rise Time:	0.9 ns
Fall Time (FWHM):	22 ns
Polarity:	pos. und neg.
Electrical Field max.:	100 kV/m
Magnetic Field max.:	265 A/m
Test Volume:	4 x 4 x 2.5 m
Pulse Repetition Rate:	1/min
Termination Resistance:	100 Ω
Dimensions L x B x H:	20 x 10 x 5 m
Standard:	VG 95371-10
Insulation / Gas:	Air, SF$_6$

A typical E-field waveform in the working volume of VERIFY is shown in Figure 5, along with an analytical curve-fit representation given by the equation

$$E(t) = E_o \Gamma \left[e^{-\alpha(t-t_s)} - e^{-\beta(t-t_s)} \right] \Phi(t - t_s).$$ (1)

The frequency domain response of this E-field is given analytically as

$$E(\omega) = E_o \Gamma \frac{(\beta - \alpha)}{(\alpha + j\omega)(\beta + j\omega)} e^{-j\omega t_s}$$ (2)

In Eq.(1), the term $\Phi(\ )$ is a unit step function and t_s is an arbitrary time shift corresponding to the turn-on time of the waveform. The appropriate parameters E_o, α, β and Γ for representing this waveform are provided in Table 4, as taken from [6]. Figure 6 presents the spectral magnitude of Eq.(2) for the VERIFY simulator.
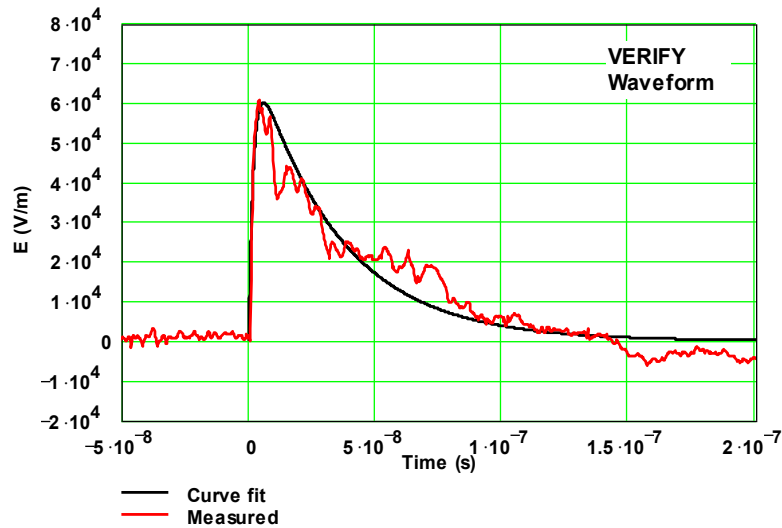
Figure 5.   Measured and curve-fit excitation waveform for the VERIFY HEMP field.

5

Table 4.   Double exponential waveform parameters for the VERIFY waveform.

Waveform	E_O (kV/m)	Γ	α (1/s)	β (1/s)
VERIFY	60	1.27	2.99×10^7	5.06×10^8
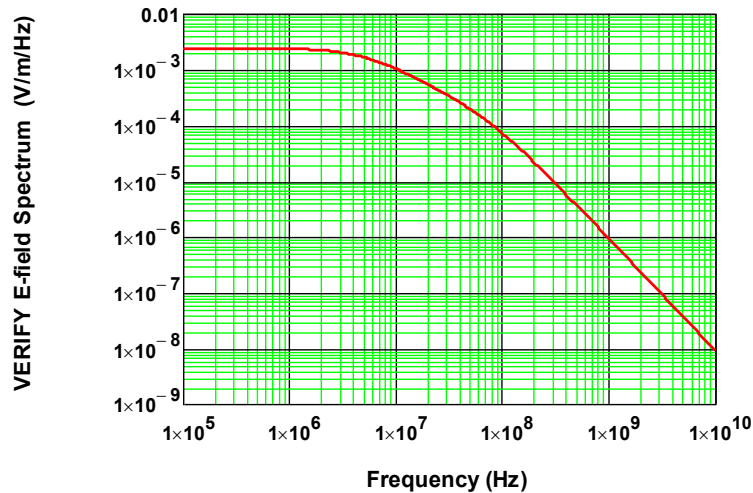
Figure 6.   E-field spectral magnitude for the VERIFY simulator.

2.4 Hyperband Antenna Systems

According to Table 1, a hyperband system is one that produces an EM environment with a band ratio (*br*) greater than 10. At the Swiss HPE Laboratory, the impulse radiating antennas (IRA) fall into this category.

The IRA is essentially a parabolic reflector antenna that is fed from a transient (pulsed) voltage source, as shown in Figure 7. This antenna is based on a standard design, which is described in ref. [7]. In this antenna there are two 400 Ω slanted transmission lines that serve as feed-arms to connect an excitation voltage source at the focus of a parabolic dish to the edge of the dish. Each feed arm is terminated in a resistance of 200 Ω at the dish edges (not shown in the diagram), and this provides a total of 400 Ω as a matched termination resistance at the ends of each of the two feed arm assemblies. Alternatively, one can consider a half-dish IRA mounted over an infinite ground plane or over a finite counterpoise platform, as shown in Figure 8.

Both the full- and half-IRA are described by the diameter of the parabolic dish, *D*, the focal length of the parabola, *F*, and the impedance ratio factor $f_g = Z_c/Z_o$, where Z_c is the characteristic impedance of the transmission line feed structure and Z_o is the free-space wave impedance. Table 5 lists these parameters for the Swiss IRA and the Swiss Half IRA, both of which will be described in more detail in Sections 2.4.1 and 2.4.2. In addition, the parameters for the non-Swiss prototype IRA and the JOLT IRA antennas are presented for completeness.
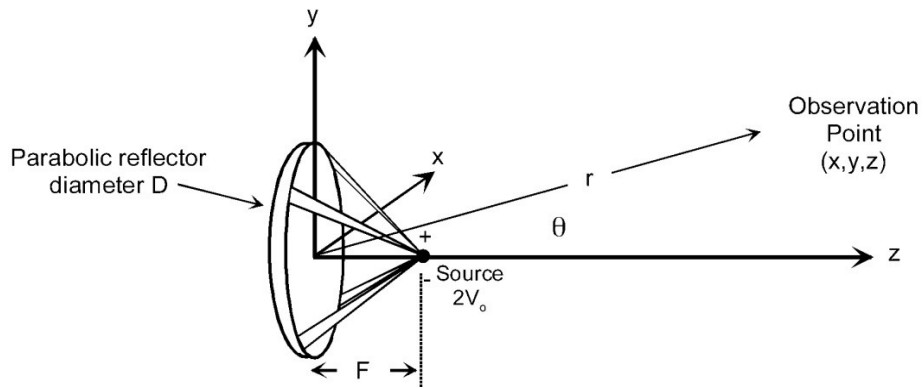
Figure 7. **The basic geometry of a full-dish IRA with four feed arms.**
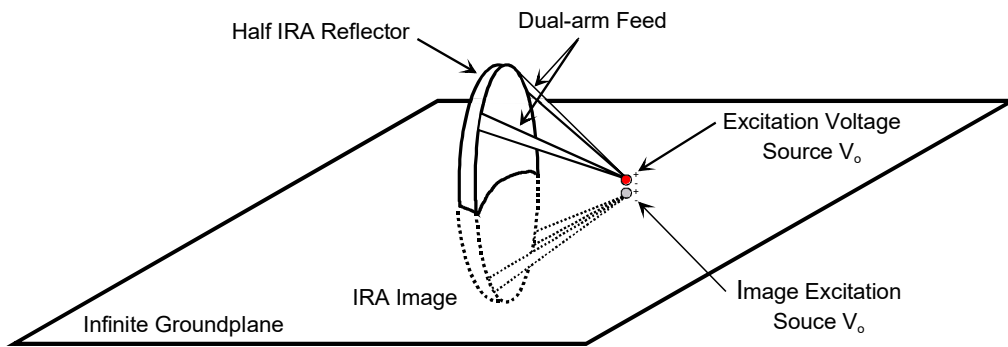
a. Half-dish IRA configuration over an infinite ground plane.
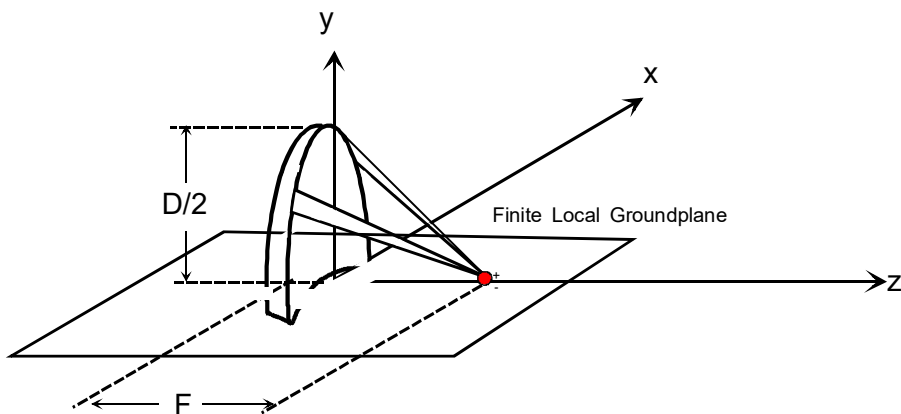
b. Half-IRA over a finite local ground plane.

Figure 8. **Geometry of the half-dish IRA.**

The radiated EM fields from an IRA can be computed using the antenna model shown in Figure 7. Results have been reported in ref. [8]. For this analysis, either an analytic solution for the transient and spectral responses for the on-axis fields is available from ref. [9], or the aperture integration approach of [8] can be used for off-axis fields.

The transient excitation of the IRA is usually provided by a high-voltage pulser that produces a fast-transient signal into the transmission line feed structure. At the antenna, the excitation is provided by the "dish voltage" sources V_o, as shown in Figure 7 and Figure 8. These sources represent the net voltage applied across the full dish and the half-dish, respectively. These voltages are initially produced by a transient pulser source V_s that is specified by the voltage waveform delivered across a standard load impedance, which is usually 50 Ω. Frequently, this voltage source is connected to the antenna source point through a transmission line containing a balun to transform the voltage into a balanced signal. In addition, the feed network might have an impedance transforming section to aid in matching the antenna impedance to that of the source. Thus, depending on the nature of the antenna feed design, the dish excitation voltage can differ from the specified pulser voltage.

To represent the pulser excitation for a wide variety of pulsers, Giri [10] has developed the following expression for the pulser voltage (delivered into a standard 50 Ω load):

$$V_s(t) = V_0\left(1+\Gamma\right)e^{-\beta\left(\frac{t-t_s}{t_d}\right)}\left[0.5\operatorname{erfc}\left(-\sqrt{\pi}\,\frac{t-t_s}{t_d}\right)u\left(-(t-t_s)\right)+\left[1-0.5\operatorname{erfc}\left(\sqrt{\pi}\,\frac{t-t_s}{t_d}\right)\right]u\left(t-t_s\right)\right] \quad (3)$$

In this expression, *erfc*(.) denotes the complementary error function and *u*(.) is the unit step (Heaviside) function. The spectrum of this voltage spectrum is given by Giri as

$$V_s(\omega) = \frac{V_0\left(1+\Gamma\right)t_d}{\left(\beta+j\omega t_d\right)}\exp\frac{1}{4\pi}\left(\beta+j\omega t_d\right)^2 \quad (\text{Volts / Hz}) \ . \quad (4)$$

The Swiss IRAs are both fed by the same pulser – a pulser from FID GmbH in Germany [11]. The prototype IRA and JOLT sources are more powerful than the FID, and consequently, they are described by Eq. (3), but with different parameters. The waveform parameters V_o, Γ, t_d and β for the sources for all four of these IRAs are provided in Table 5.

Table 5.   Dimensions and waveform parameters for various IRA antennas

	Prototype IRA	JOLT (USA)	Swiss IRA	Swiss Half IRA
Antenna Parameters				
D (m)	3.658	3.048	1.8	1.41
F (m)	1.218	1.219	0.482	0.376
f_g (unitless)	1.061	1.061	1.061	1.061
Waveform Parameters				
V_o (kV)	120	1000	10	10
Γ (unitless)	0.006	0.025	0.24	0.24
t_d (ps)	100	180	140	140
β (unitless)	0.006	0.036	0.25	0.25

2.4.1 The Swiss Impulse Radiating Antenna (SWIRA)

The <u>Sw</u>iss <u>i</u>mpulse <u>r</u>adiating <u>a</u>ntenna (SWIRA) is a hyperband antenna that has been used for testing both facilities and equipment. It is shown in Figure 9.

Figure 9.   Photo of the Swiss IRA.

The pertinent dimensions of this antenna and the excitation voltage parameters have been listed in Table 5, and the following is a list of features for this antenna:

Table 6.   Properties of the SWIRA antenna.

Band:	Hyperband
Frequency range:	0.1 – 3.5 GHz
Input Impedance:	50 Ω
Polarity:	bipolar
Polarization:	horizontal
Max. applicable Voltage:	10 kV
Sources:	FID, Grant…
Directivity:	~5°
Pulse Repetition Rate:	1 Hz to 50 kHz
Standard:	IEC 61000-2-13
Insulation / Gas:	Dielectric, Air

The earlier descriptions of the radiated field spectra for the prototype IRA and JOLT have used an observation distance of 100 meters from the antenna. To provide a consistent comparison with these other environments, the SWIRA environment is also calculated and displayed at 100 meters. Figure 10 shows the transient E-field for the FID pulser excitation, and the corresponding spectral magnitude is shown in Figure 11. It should be noted that this antenna uses a balun to provide balanced excitation voltage to the dish, and hence, the antenna dish voltage is twice the specified pulser voltage.

9
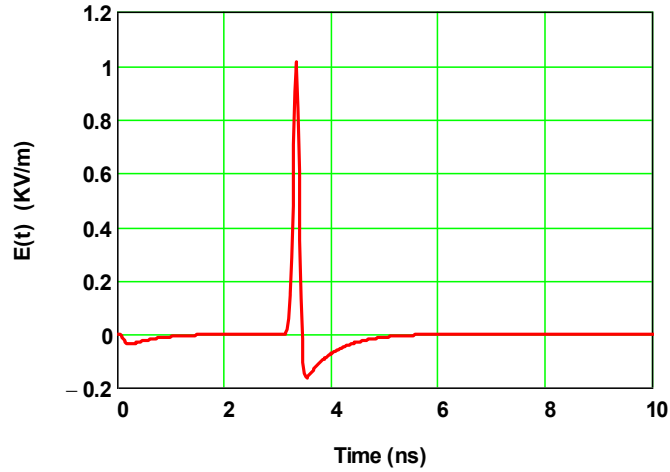
Figure 10. On-axis transient E-field from the SWIRA at a range of 100 m.
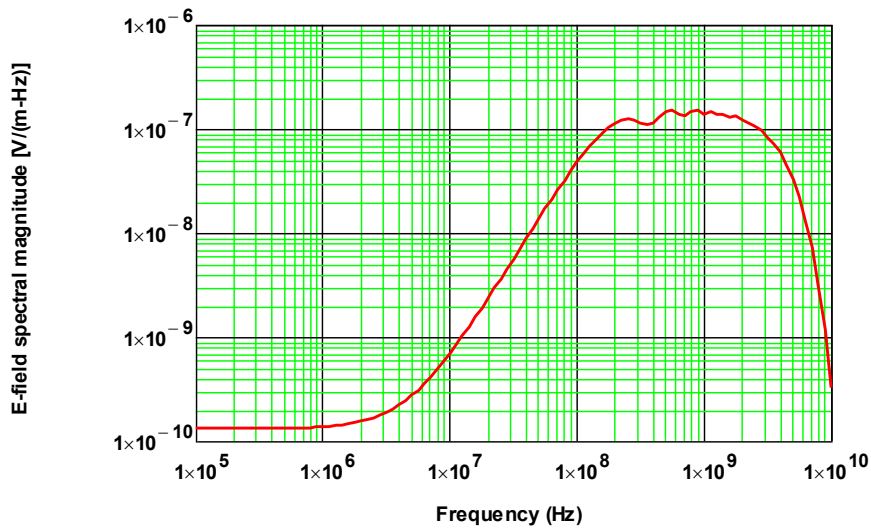
Figure 11. Spectral magnitude of the on-axis E-field from the SWIRA at a range of 100 m.

2.4.2 The Swiss Half-IRA (SWHIRA)

The <u>Sw</u>iss <u>h</u>alf <u>i</u>mpulse <u>r</u>adiating <u>a</u>ntenna (SWHIRA) is a half-dish version of the full IRA. It is displayed in Figure 12.

This antenna can be fed by the UWB FID pulser as in the case of the full IRA, or by any number of other moderate-band or ultra moderate-band sources. The operational characteristics of this antenna are presented in Table 7 and Table 5 provides the pertinent dimensions of the antenna, as well as the FID pulser waveform parameters for use in Eqs.(3) and (4).

10
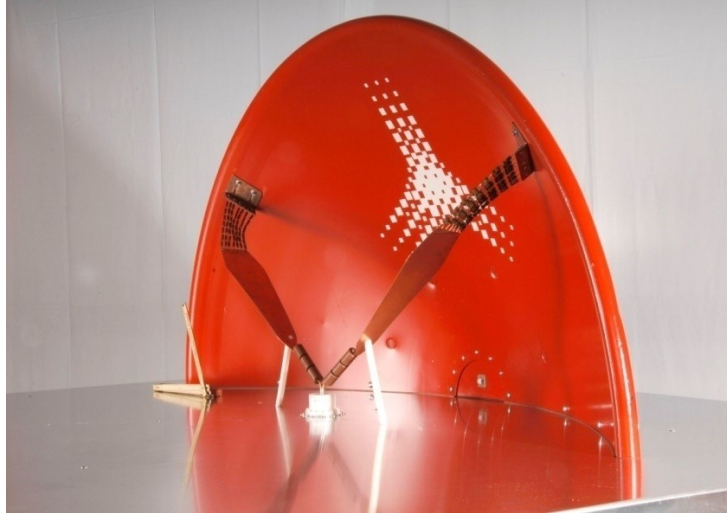
Figure 12.   Photo of the Swiss half-IRA.

Table 7.   Properties of the SWHIRA antenna.

Design and build:	2006
Band:	Hyperband
Frequency Range:	0.12 – 4 GHz
Input Impedance:	50 / 100Ω
Polarity:	bipolar
Polarization:	vertical
Max. applicable Voltage:	30 kV
Sources:	FID/Oscillator
Directivity:	~5°
Dimension Ø:	1.4 m
Standard:	IEC 61000-2-13
Insulation / Gas:	Air, Dielectric

Figure 13 plots the radiated on-axis transient E-field from this antenna, at a range of 100 meters for the FID pulser excitation. The corresponding spectral magnitude for the E-field with the FID excitation is shown in Figure 14.

For this antenna, the 50 Ω output of the pulser is connected to the input of the antenna (100 Ω) through an impedance transition section. No balun is required in this case.
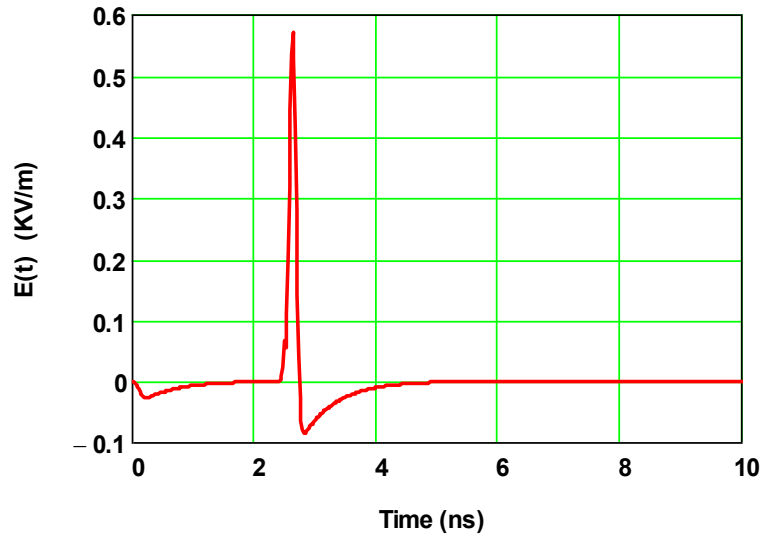
Figure 13. On-axis transient E-field from the SWHIRA at a range of 100 m.
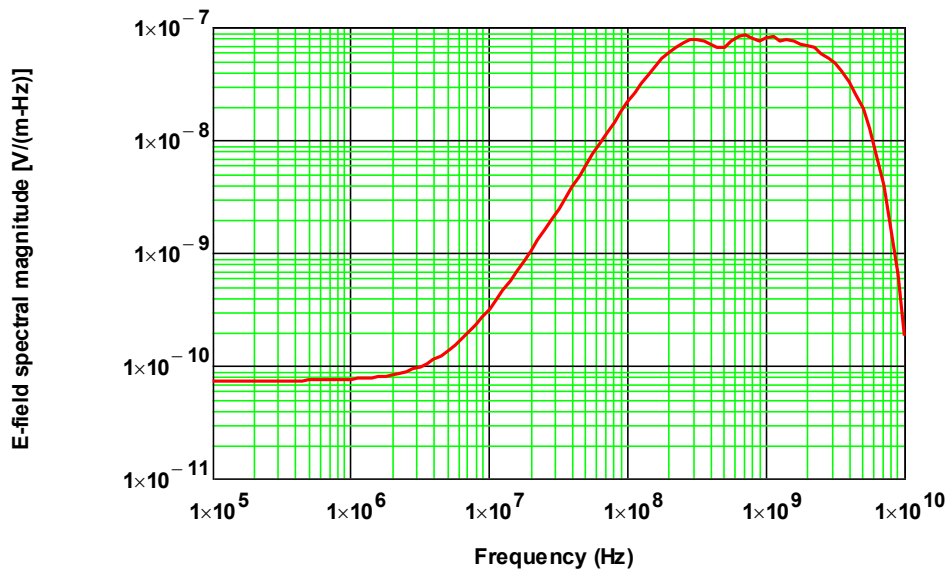
Figure 14. Spectral magnitude of the on-axis E-field from the SWHIRA at a range of 100 m.

2.5 Moderate or Meso Band Antenna Systems

A properly designed helix antenna is an example of a mesoband antenna that can be used for radiating signals that have smaller band ratios than found in the mesoband IRAs. Such an antenna has been discussed and analyzed in ref. [12].

This type of antenna is typically used with a pitch angle between 12 to 14 degrees. The length of one turn of the helix is the quadrature sum of the circumference of one turn and the spacing S between turns. The helix parameters are chosen so such that the length of one turn of the helix is about 1 wavelength at the specified operational frequency. For this design, the radiation pattern from the antenna is a narrow beam emitted along the antenna axis and is nearly constant as the frequency changes in a relatively small band of frequencies around the design frequency.

A design for such an antenna with an operational frequency of 500 Hz has been developed and built by D. V. Giri for the HPE Laboratory in Spiez. The basic geometry of this antenna is shown in Figure 15. The conductor for the antenna is wound in a helical manner around the z-axis and is fed against the disk ground plane by coaxial cable from the backside of the ground. This is equivalent to having a small voltage source feed located at the wire-ground plane junction.
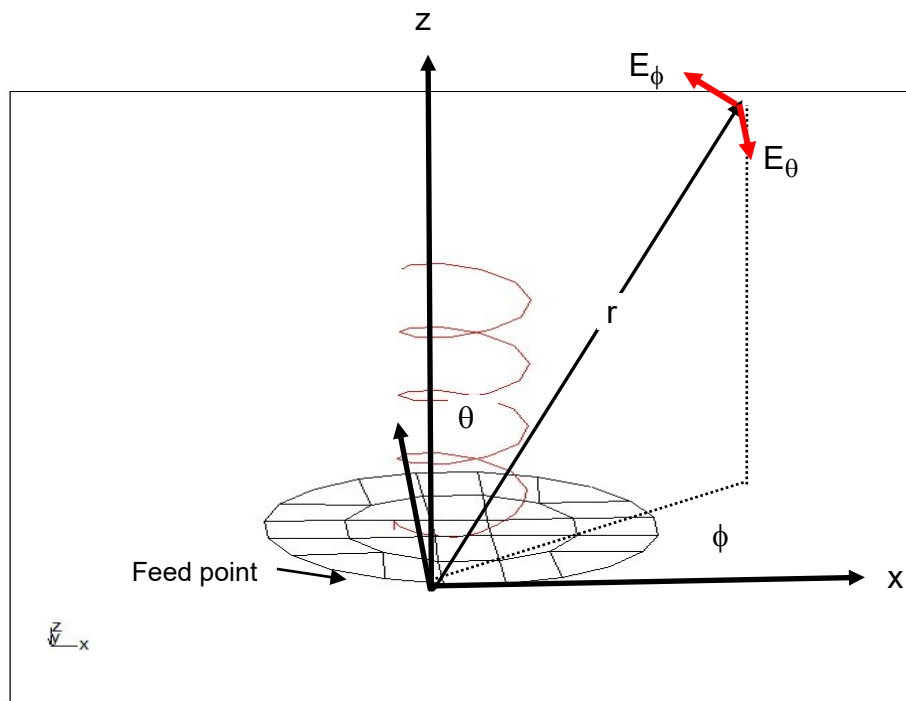
Figure 15.   The helix antenna and the coordinate system for analyzing the radiated field.

In ref. [13], the behavior of the helix antenna is described in more detail and the far-field radiation pattern and frequency dependence is calculated. Design parameters for helix antennas operating at 500 and 200 MHz are provided in this reference. Table 8 summarizes the helix parameters used for these designs.

The vector components of the normalized on-axis E-field spectrum produced by a helix antenna are shown in Figure 16. These plots illustrate the normalized transfer functions

13

rE_θ/V and rE_ϕ/V, where V denotes the voltage source strength that excites the antenna. Upon multiplying these transfer functions by the spectrum of the voltage exciting the antenna, the radiated E-field can be calculated. For the helix antenna, it is found that the on-axis E-field is nearly circularly polarized, which implies that both E_θ and E_ϕ are present in the far field, and that they are 90 degrees out of phase. The particular curves shown in Figure 16 are for the 500 MHz helix antenna, but the behavior of the spectra are typical of other helix designs having a similar geometry.

Table 8.   Parameters for the Swiss Helix Antennas Designed for 200 and 500 MHz.

Helix Parameter	f = 500 MHz	f = 200 MHz
Major diameter (D) (center to center of conductor)	19.05 cm	47.62 cm
Circumference (C) = 3.1415 x D	59.84 cm	1.50 m
Minor diameter of conductor ($2r$)	9.52 mm	23.81 mm
Minor radius of conductor (a)	4.762 mm	11.91 mm
Spacing between adjacent turns (S)	13.33 cm	33.34 cm
Length L of one turn (approximately one wavelength at design frequency)	61.31 cm	153.28 cm
Free-space wavelength at design frequency	60 cm	1.50 m
Number of turns N	10	10
Total axial length L_t = $N\,S$ = 10 S	1.33 m	3.33 m
Pitch angle θ_p = arctan (S/C)	12.56°	12.56°
Ground plane is an octagon made from a square metal plate	55.88 cm x 55.88 cm	1.4 m x 1.4 m.

In the following subsections we provide additional response data that are specific to the Swiss 500 MHz and 200 MHz antennas.
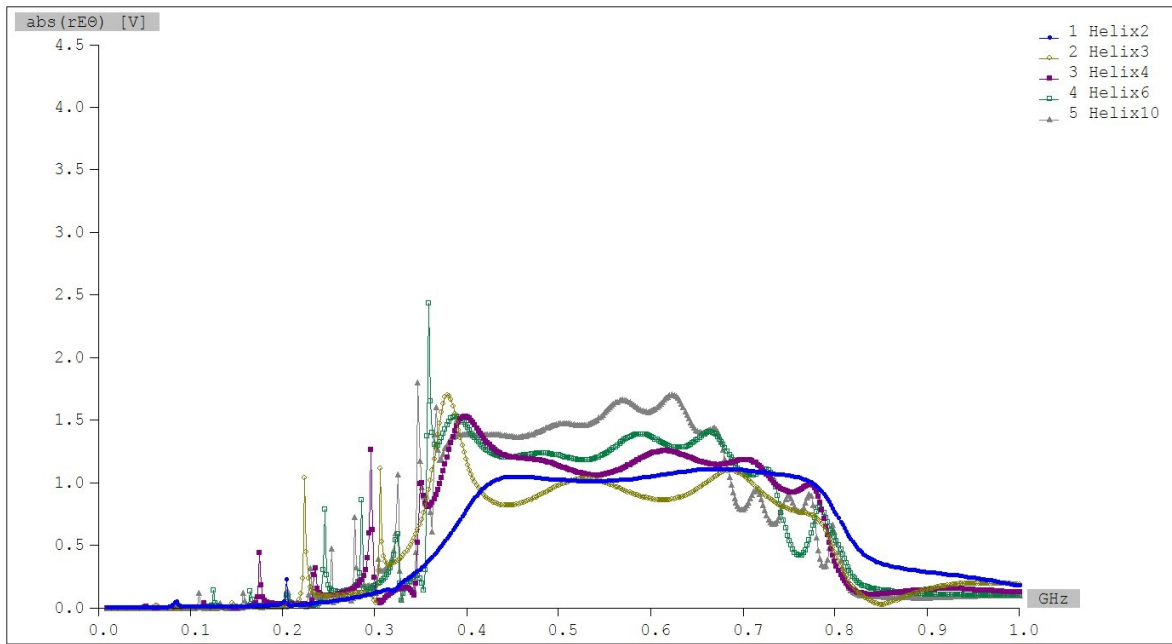
a. $|rE_\theta/V|$
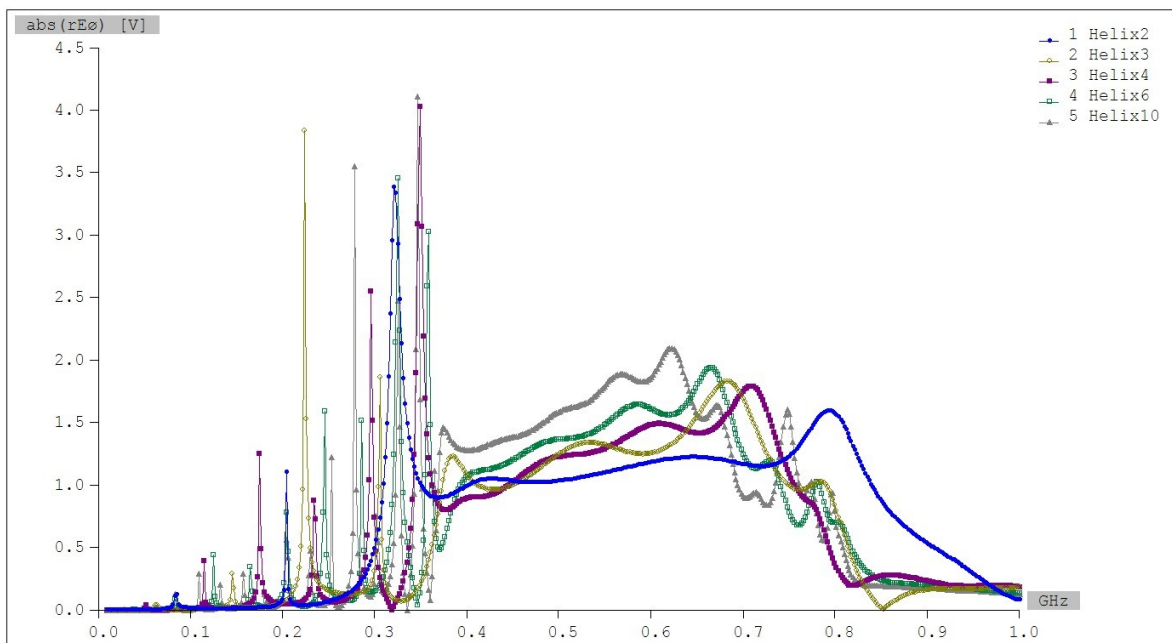
b. $|rE_\phi/V|$

Figure 16. **Plots of the frequency dependence of the normalized on-axis radiation patterns $|rE/V|$ for the θ and ϕ components of the E-field, for different numbers of turns of the helix antenna. (Turns are indicated in the name of the data files in the plot.)**

2.5.1 500 MHz Swiss Helix Antenna

The 500 MHz Swiss Helix Antenna is a mesoband antenna which has recently been used in a HPEM effects test program [14]. This antenna is pictured in Figure 17.

Figure 17.   Photo of the 500 MHz Swiss Helix Antenna.

The design of this antenna was developed by Dr. D. Giri, and it has the following characteristics [15]:

Specification of the Antenna:

Purchased:	2007
Band:	Mesoband
Frequency Range:	400 – 600 MHz
Input Impedance:	50 Ohm/Open Circuit
Polarity:	bipolar
Polarization:	circular
Max. applicable Voltage:	30 kV
Sources:	CW/Oscillator…
Directivity:	~ 20°
Dimensions L /Ø:	1.3m / 0.6m
Standard:	IEC 61000-2-13
Insulation / Gas:	Air, Dielectric

The source for this antenna consists of a high-pressure hydrogen insulated 3.7 Ω coaxial transmission line, which serves as a resonant circuit element. It is charged by a DC voltage source (typically about 30 kV) and then is discharged by closing the high-pressure nitrogen switch integrated into the left end of the oscillator. Figure 18 provides an illustration of this source, isolated from the helix antenna and ground plane.
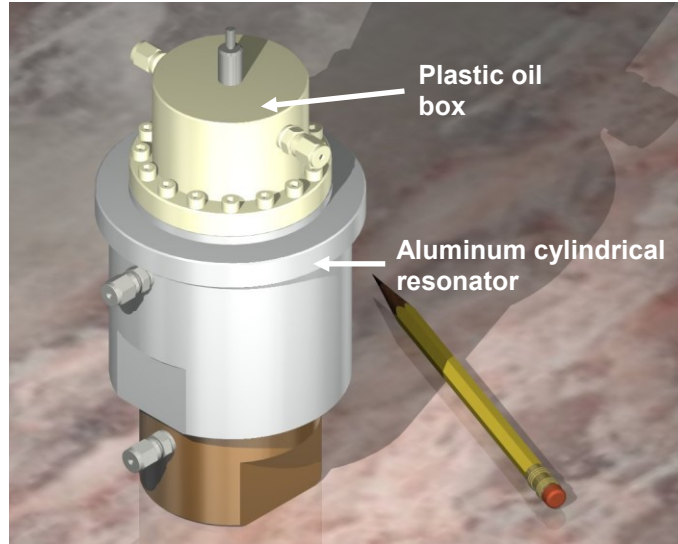
Figure 18.   **The structure of the 500 MHz oscillator**

The source output voltage $V(t)$ into the 100 Ω load can be modeled adequately by an exponentially damped sine wave of the form

$$V(t) = Ae^{-\alpha(t-t_s)} \sin\left(2\pi f_o\left(t-t_s\right)\right)\Phi\left(t-t_s\right) \tag{5}$$

where f_o is the oscillation frequency of 500 MHz, t_s is an arbitrary time shift or "start time" of the waveform, and α is the damping constant of the waveform given by

$$\alpha = \frac{\pi f_o}{Q} \tag{6}$$

with Q being the *quality factor* of the signal. Typically, Q ranges from 1 to 100, depending on the losses in the oscillator and the nature of the load resistance.

Figure 19 presents the measured range-normalized transient electric field components for the 500 MHz helical antenna [14]. In comparing these waveforms with calculated responses with differing pulser amplitudes and Qs, it is estimated that the pulser waveform is best described by the parameters $Q = 7$ and $V_{ant} = 13$ kV.

For these parameters, the computed E-field spectrum produced by this helix antenna at a range of 100 m is shown in Figure 20. Note that this is the *total* E-field spectrum, which combines both the E_x and E_y field components.
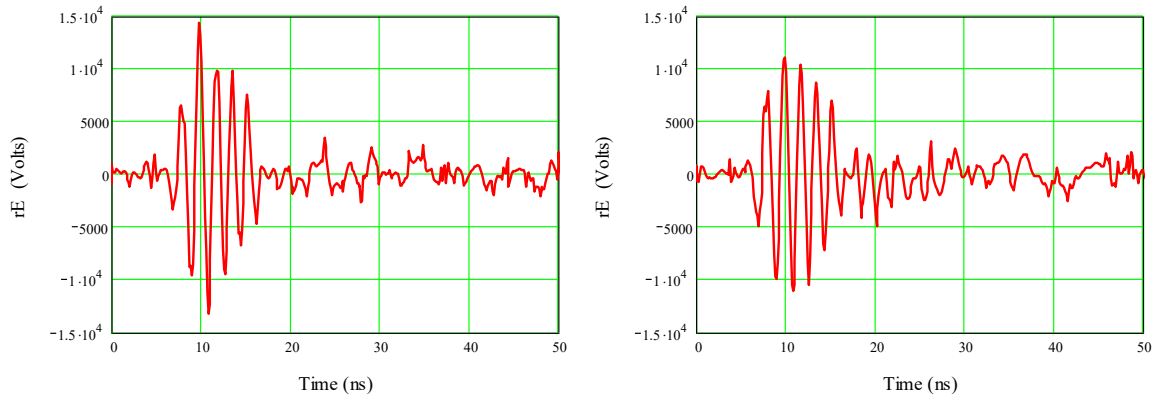
a. E_x component   b. E_y component

Figure 19. **The measured range-normalized transient electric fields of the 500 MHz helical antenna. (a)** E_x **component, and (b)** E_y **component.**
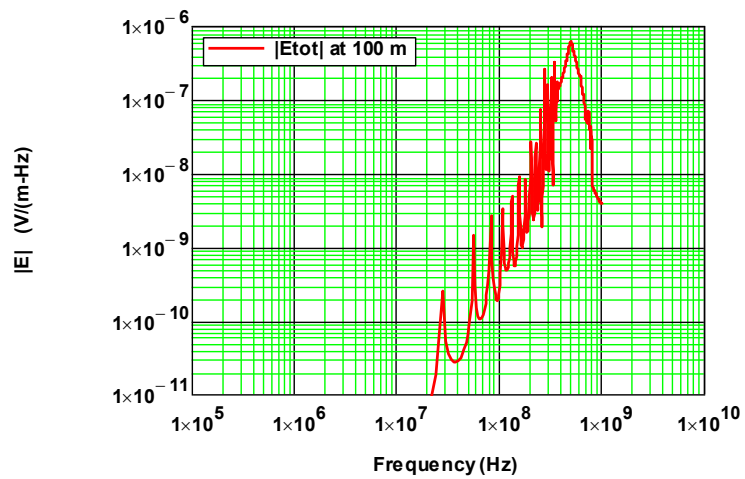
Figure 20. **Spectral magnitude of the total radiated electric field at 100 m from the 500 MHz helix antenna.**

2.5.2 200 MHz Swiss Helix Antenna

For the 200 MHz moderate band source, the SSO-200, a lower frequency helical antenna has been procured, and it should be operational at the HPE Laboratory shortly. Presently, we do not have field measurements for this antenna. However, the radiated fields from the 500 MHz antenna can be scaled in frequency to yield a good estimate of the expected radiation from this antenna.

A photograph of the 200 MHz antenna is shown in Figure 21.

Figure 21.   The helical antenna for a center frequency of 200 MHz.

The antenna in Figure 21 has a 50 Ω connector at its input, and the input impedance of the helix must be suitably transformed to yield this value. This is done by shaping the initial part of the first turn of the helix structure to minimize the S_{11} parameter of the antenna over the frequency band of operation of the antenna. We have measured and optimized S_{11} at the input connector, and the result is shown in Figure 22.
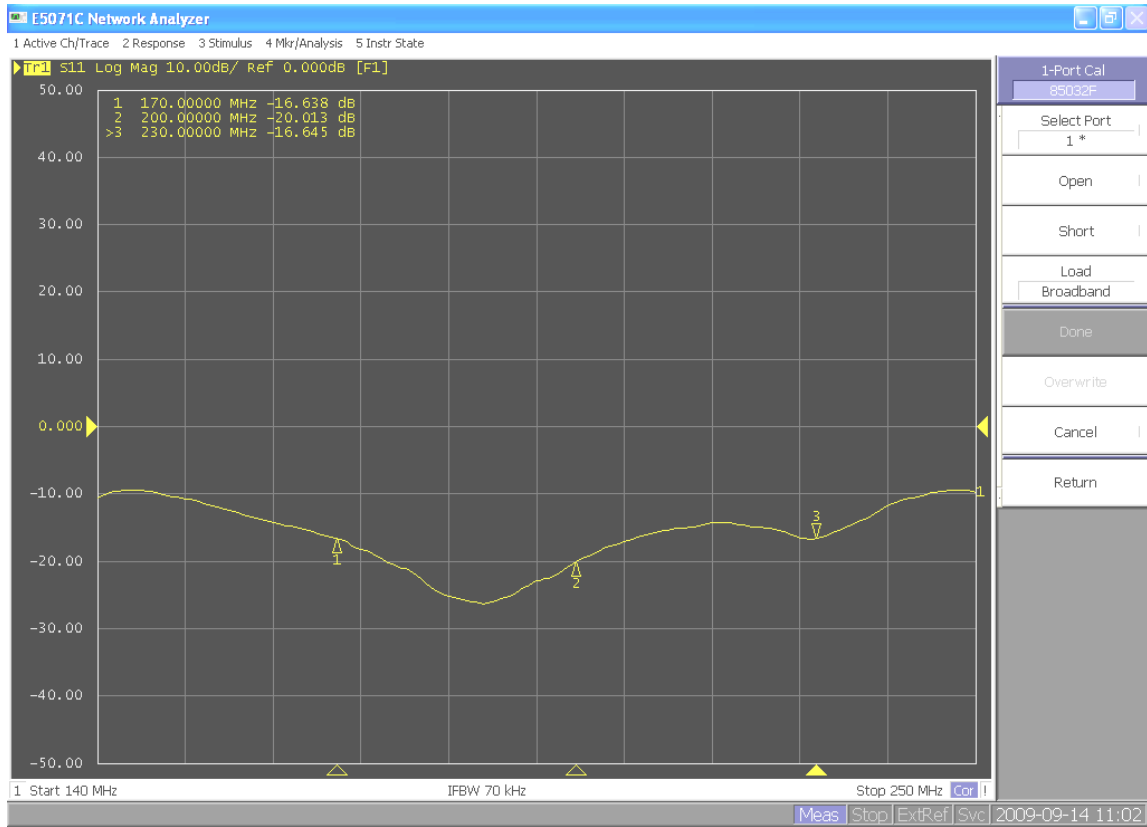
Figure 22.   *S$_{11}$* **measurement at the input of the 200 MHz helical antenna.**

In Figure 22 we see that *S$_{11}$* is better than –15 dB in the frequency range of 170 MHz to 230 MHz. The three markers 1, 2 and 3 in this figure correspond to the frequencies of 170 MHz, 200 MHz and 230 MHz. This antenna has been delivered to the HPE laboratory, and it should be integrated with the SSO-200 and characterized soon.

2.6 Narrowband Systems

2.6.1 2.4 GHz Klystron/Horn System

A readily available CW microwave source in the S-band is the magnetron device found in a microwave oven (see Figure 23). The microwave oven used here was rated at a microwave output of 800 W, at a frequency of 2.45 GHz. The microwave power from the magnetron is extracted into a standard rectangular waveguide. We found that the rectangular waveguide in the commercial oven was a non-standard (not 2 to 1 in its aspect ratio) waveguide.

Figure 23.   Power extraction from a microwave oven using a WR-340 Waveguide.

We experimented have with three different antennas and all of these are available at the HPE Laboratory for testing purposes. These antennas include:

- An open-ended WR-340 waveguide,
- a pyramidal horn antenna, and
- a reflector antenna fed by open-ended waveguide.

Each of the above antennas was analyzed and their radiation patterns computed. The mathematical expressions are well known. The computed radiation patterns for the three antennas are shown in Figure 24 through Figure 27.
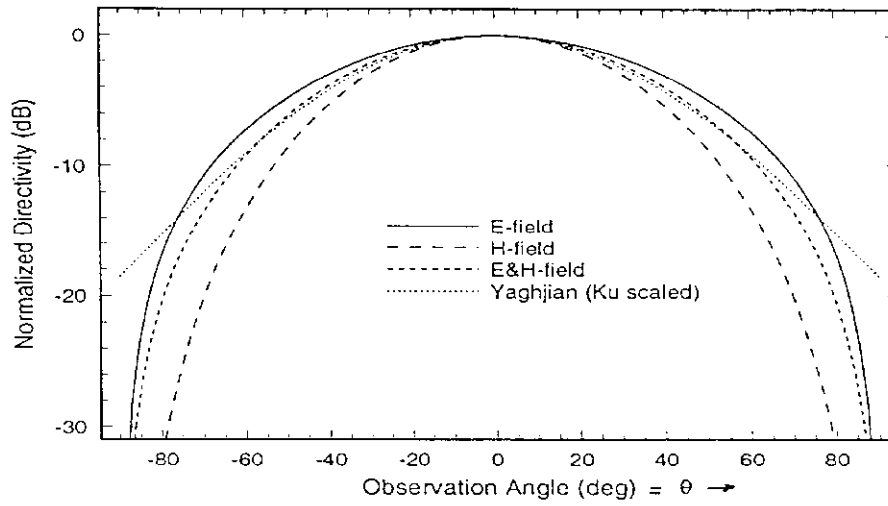
Figure 24. **E-plane (φ = 90°) radiation pattern of the open-ended WR-340 waveguide.**
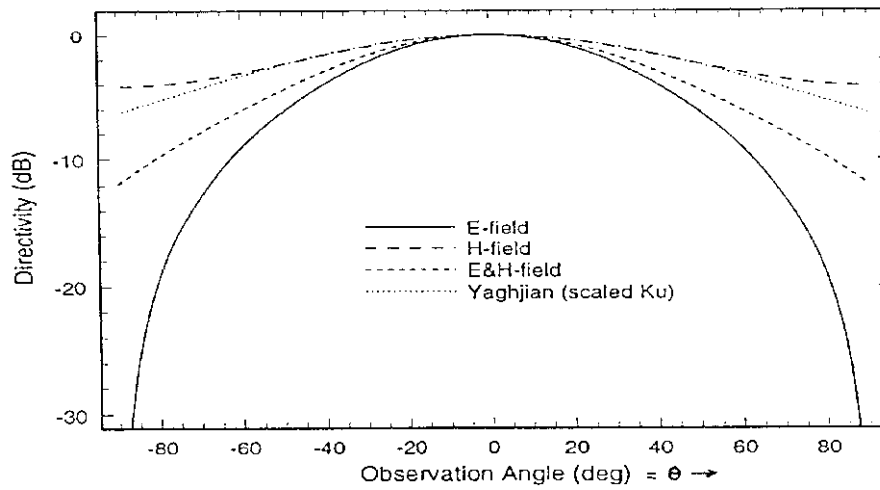
Figure 25. ***H*-plane (φ = 0°) radiation pattern of the open-ended WR-340 waveguide.**
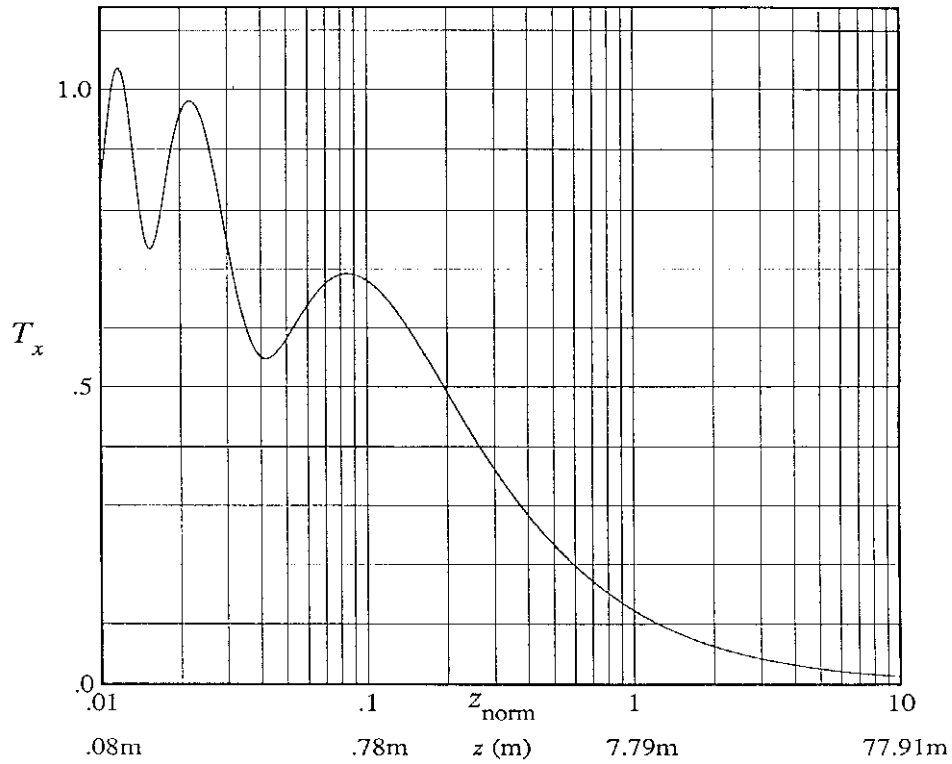
Figure 26.   Near and far fields from the pyramidal horn.
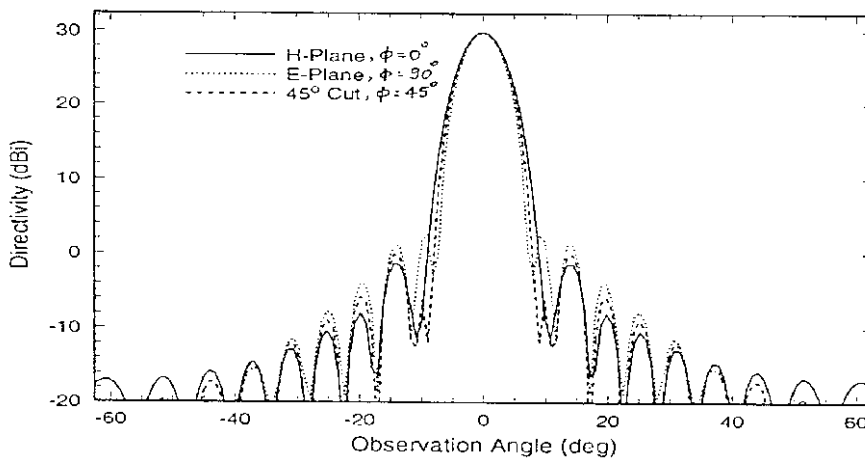
Figure 27.   Radiation pattern of the reflector antenna (1.4 m diameter), illuminated by the WR-340 open-ended waveguide,

These three antennas have been built at the laboratory, and are shown in Figure 28 through Figure 30. Measurements of the EM fields produced by these radiators are in good agreement with the computed results.

23
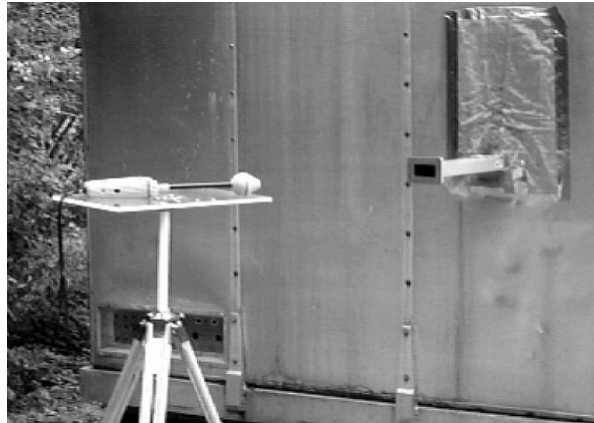
Figure 28.   Photo of the open-ended WR-340 waveguide radiator.
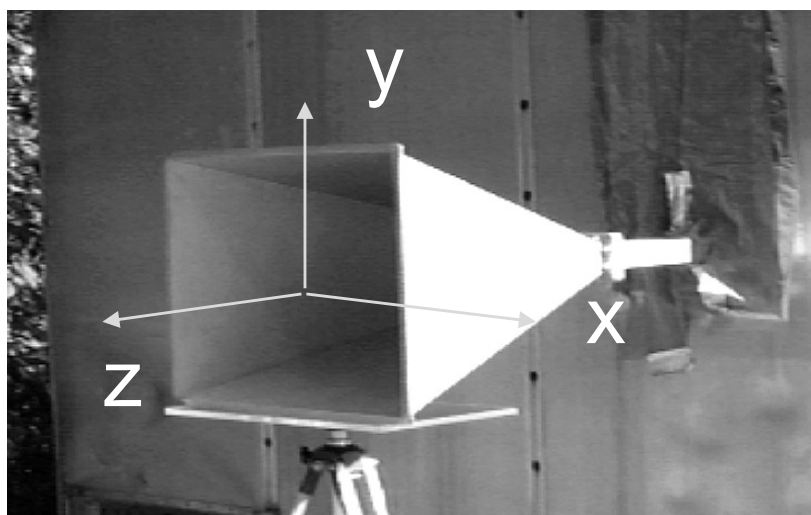
Figure 29.   Photo of the pyramidal horn antenna at 2.4 GHz.
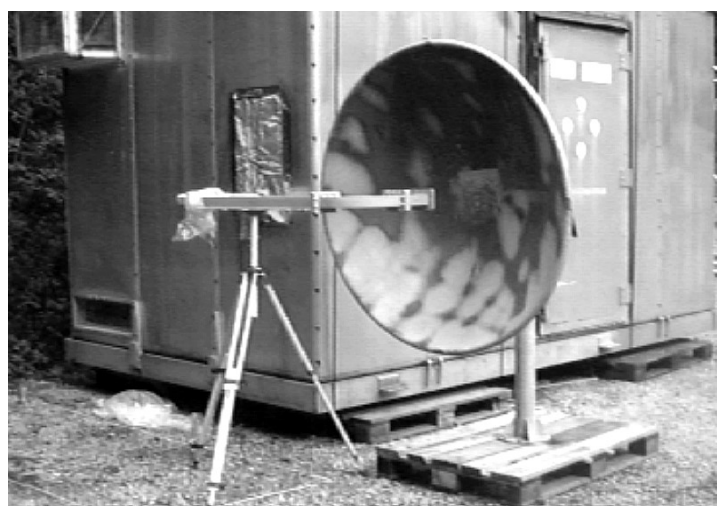
Figure 30.   Photo of the reflector antenna fed by open-ended waveguide

24

Although, this study primarily focused on extracting the power from the magnetron source and efficiently radiating it, we also attempted some simple coupling measurements with test objects such as:

- Medium wave (AM), FM radios,
- Swiss swatch watches,
- Small pellet explosives,
- Calculators (hand held),
- A wild mushroom,
- Absorbing material, and
- Fluorescent lamp.

All of the above-mentioned test objects had observable effects at various distances in the range of 0.5 to 6 m. No systematic effects testing was done and are possible in the future, perhaps with even higher microwave power. The observed effects with the present ~ 1 kW CW source was:

- the wrist watch was totally damaged,
- mushroom started to smoke (water content),
- radio showed thermal damage,
- pellet-explosive exploded when the leads were turned into a half wave dipole receiver,
- calculators were damaged and some of the leads going to the LED display were burnt,
- the absorbing material, in front of the radiators experienced heating and the rise in temperature was apparent with the 10 second exposure, and
- The fluorescent lamp emitted light.

3. Update of the HPEM Environment Chart

Using the data on the Swiss HPEM sources described in Section 2, we have compiled these into a single spectral chart, similar to that of Figure 1. This overlay spectral plot is shown below in Figure 31.

Figure 32 presents an update of the 2007 chart showing other HPEM source spectra worldwide. This is a slight revision of the chart provided in ref. [3].
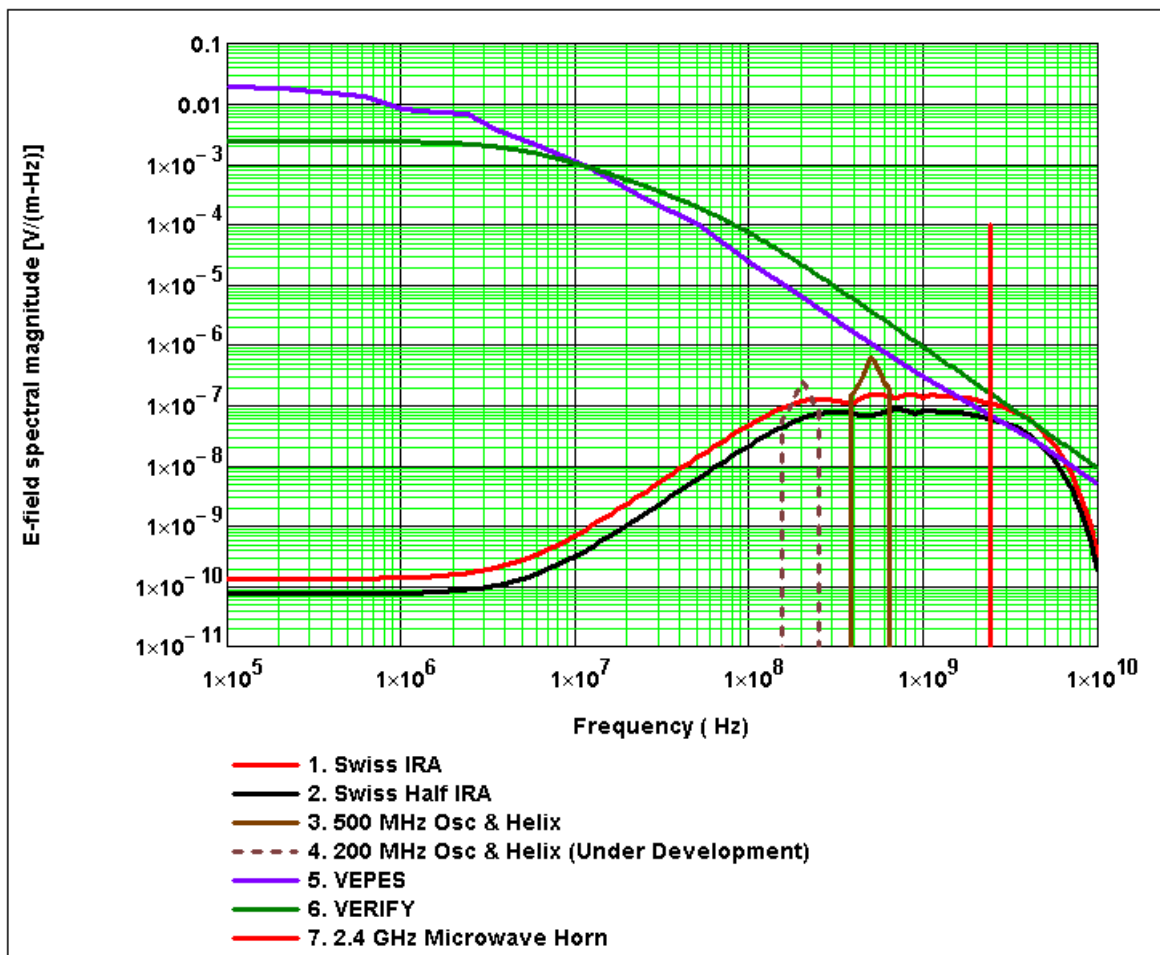
Figure 31.   An overlay comparison of the HPEM spectra for the sources available at the Swiss HPE Laboratory, as of 2009.
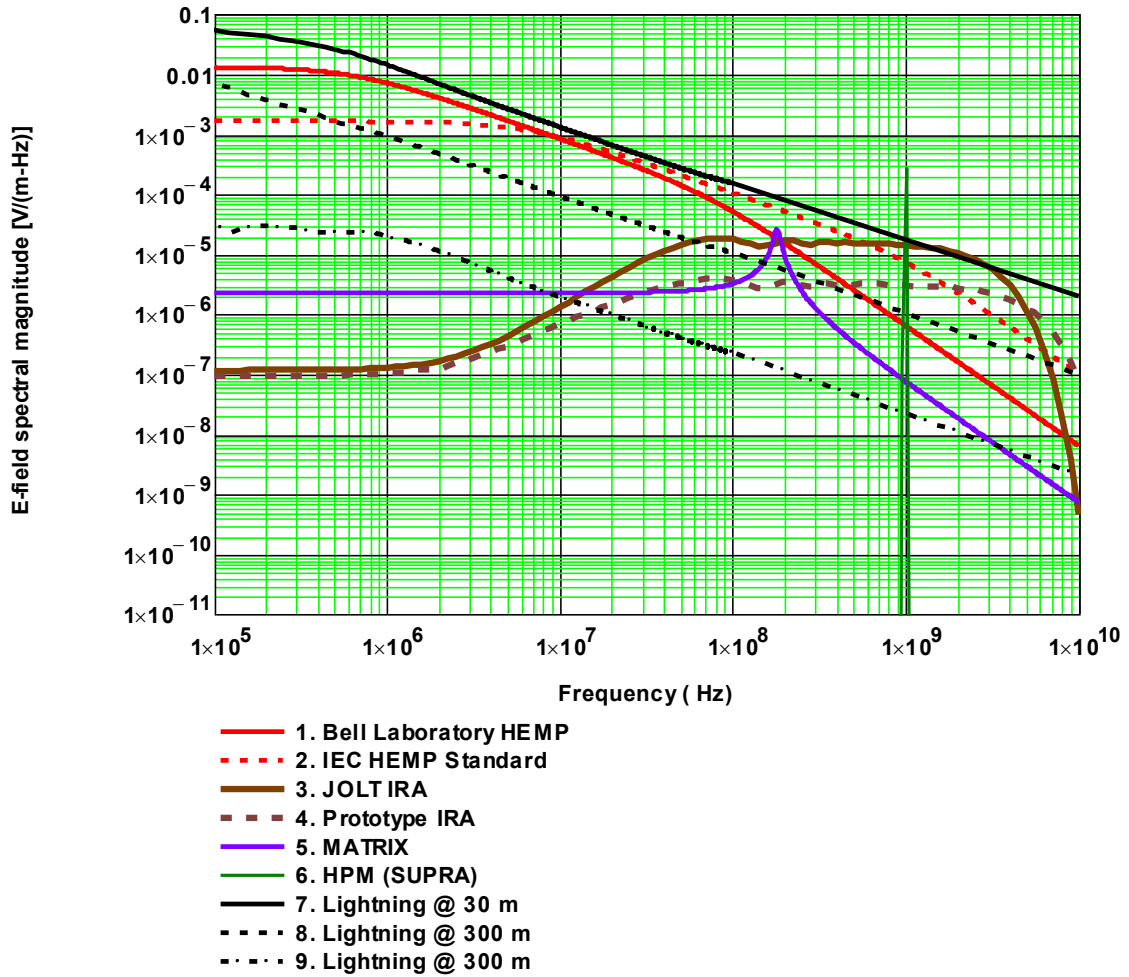
Figure 32. **Revision of the HPEM spectral plot of Figure 1, as provided by ref.[3].**

4. Summary

In this report, the HPEM systems available at the HPE laboratory, consisting of sources and antennas or transmission lines have been described. They consist of HEMP simulators (ex: VEPES and VERIFY), narrowband systems (ex: 2.4 GHz magnetron source with different antennas), Mesoband systems at 200 MHz and 500 MHz with helical antennas and finally hyperband systems with half and full IRAs.

It is noted that the vertically polarized HEMP is well simulated by the existing simulators, which are currently operational. The other HPEM systems have limitations, in the sense that the achievable EM field levels are relatively low in amplitude.

This compendium can be updated as future systems are procured at the HPE laboratory.

5. References

1.   Giri, D. V., and F. M. Tesche, "Classification of Intentional Electromagnetic Environments (IEME*)", IEEE Transactions on EMC*, August 2004, Vol. 46; Part 3, pp 322-328.

2.   Giri, D. V. and A. W. Kälin, "Many Faces of HPEM", Presented at the AMEREM 1996 Meeting, University of New Mexico, Albuquerque, NM, July 1996.

3.   Giri, D. V., F. M. Tesche, and A. W. Kälin, "Comparative Study of High-Power Electromagnetic (HPEM) Environments", Presented at the URSI 2007 North American Radio Science Meeting, Ottawa, ON, Canada, July 22 - 26, 2007.

4.   International Standard IEC 61000-4-32, Electromagnetic Compatibility (EMC) – Part 4-32: Testing and Measurement Techniques – High-altitude Electromagnetic Pulse (HEMP) Simulator Compendium, First Edition, October 2002.

5.   Tesche, F. M., "Discussion of the HEMP Environment in the Modified VEPES Simulator", report prepared for **armasuisse** contract 8003401055, HPEM-Labor, Spiez, Switzerland October 10, 2007.

6.   Tesche, F. M., "Additional Electromagnetic Shielding Studies for Enclosures", Report for armasuisse Contract 4500312242, September 19, 2004.

7.   Farr, E., "Development of a Reflector IRA and a Solid Dielectric Lens IRA, *Sensor and Simulation Note 396*, April 1996.

8.   Tesche, F. M., "Swiss Impulse Radiating Antenna (SWIRA) Characterization", report prepared for **armasuisse** contract 4500314446, HPEM-Labor, Spiez, Switzerland, August 8, 2005.

9.   Oleg V. Mikheev, et. al., "New Method for Calculating Pulse Radiation from an Antenna with a Reflector", *IEEE Trans EMC*, Vol. 39, No. 1, February 1997.

10.   D. V. Giri, J. M. Lehr, W. D. Prather, C. E. Baum, and R. J. Torres, "Intermediate and Far Fields of a Reflector Antenna Energized by a Hydrogen Spark-Gap Switched Pulser", *IEEE Trans. Plasma Science*, Oct. 2000.

11.   http://www.fidtechnology.com/

12.   Tesche, F. M., "Generation of High-Power Transient Waveforms using a Wideband Amplifier and an Arbitrary Waveform Generator", Report prepared for **armasuisse** contract 8003405510, Sept. 17, 2008, revised Sept. 19, 2008.

13.   Tesche, F. M., "Comments on the Radiation of the Swiss Helix Antenna with Different Numbers of Turns", report prepared for **armasuisse** contract 8003401055, HPE-Labor, Spiez, Switzerland, September 22, 2007

14.   Tesche, F. M and D. V. Giri, "Test Program for the Demonstration of High Power Electromagnetics (HPE) Effects: Volume I – Test Planning and Volume II – Test

Results", report prepared for **armasuisse** contract 8003401055, HPEM Technical Support 2007, HPE-Labor, Spiez, Switzerland October 12, 2007.

15. Giri, D.V., "Design of 30kV, 500 MHz Switched Oscillator", Pro-Tech final report (briefing format) for armasuisse contract, 2006.